Flavor stability of a realistic accretion-phase supernova neutrino flux

Srdjan Sarikas,[1,2] Georg G. Raffelt,[2] Lorenz Hüdepohl,[3] and Hans-Thomas Janka[3]

[1] *Dipartimento di Scienze Fisiche, Università di Napoli Federico II, 80126 Napoli, Italy*
[2] *Max-Planck-Institut für Physik (Werner-Heisenberg-Institut), Föhringer Ring 6, 80802 München, Germany*
[3] *Max-Planck-Institut für Astrophysik, Karl-Schwarzschild-Str. 1, 85748 Garching, Germany*

(Dated: 15 September 2011)

Self-induced flavor conversions of supernova (SN) neutrinos can strongly modify the flavor dependent fluxes. We perform a linearized flavor stability analysis with accretion-phase matter profiles of a $15\,M_\odot$ spherically symmetric model and corresponding neutrino fluxes. We use realistic energy and angle distributions, the latter deviating strongly from quasi-isotropic emission, thus accounting for both multi-angle and multi-energy effects. For our matter and neutrino density profile we always find stable conditions: flavor conversions are limited to the usual MSW effect. In this case one may distinguish the neutrino mass hierarchy in a SN neutrino signal if the mixing angle Θ_{13} is as large as suggested by recent experiments.

PACS numbers: 14.60.Pq, 97.60.Bw

Introduction.—The huge neutrino fluxes emitted by core-collapse supernovae (SNe) are key to the explosion dynamics and nucleosynthesis [1] and detecting a high-statistics "neutrino light curve" from the next nearby SN is a major goal for neutrino astronomy [2–4]. Besides probing the core-collapse phenomenon in unprecedented detail, one may detect signatures of flavor oscillations and extract information on neutrino mixing parameters [5].

The refractive effect caused by matter [6] suppresses flavor oscillations until neutrinos pass through the MSW region in the collapsing star's envelope [7, 8]. However, neutrino-neutrino interactions, through a flavor off-diagonal refractive index [9, 10], can trigger self-induced flavor conversions [11–13]. This collective effect usually occurs between the neutrino sphere and the MSW region and can strongly modify neutrino spectra [14–16], although this would never seem to help explode the star [17]. Actually, in low-mass SNe (not studied here) the density falls off so fast that MSW can occur first, leading to novel effects on the prompt ν_e burst [18–20].

Collective oscillations at first seemed unaffected by matter because its influence does not depend on neutrino energies [14]. However, depending on emission angle, neutrinos accrue different matter-induced flavor-dependent phases until they reach a given radius. This "multi-angle matter effect" can suppress self-induced flavor conversion [21]. Based on schematic flux spectra, this was numerically confirmed for accretion-phase SN models where the density near the core is large [22]. This epoch, before the delayed explosion finally takes off, is when the neutrino luminosity and the difference between the $\bar\nu_e$ and $\bar\nu_{\mu,\tau}$ fluxes are largest. If self-induced flavor conversion did not occur and the mixing angle Θ_{13} was not very small [23], the accretion phase would provide a plausible opportunity to determine the mass hierarchy [5, 22].

Numerical multi-angle simulations of collective oscillations are very demanding [24], but it is much easier to study if such oscillations are suppressed for given density profile and neutrino distributions. Self-induced conversion requires that part of the spectrum is prepared in one flavor, the rest in another. The collective mode consists of pendulum-like flavor exchange between these parts without changing the overall flavor content [11, 25–27]. The inevitable starting point is a flavor instability of the neutrino distribution caused by neutrino-neutrino refraction. An exponentially growing mode can be detected with a linearized analysis of the evolution equations [13, 28]. We here apply this method to a numerical accretion-phase SN model, for the first time using both realistic neutrino energy spectra and angular distributions.

Numerical SN model.—Our spherically symmetric simulation to produce an accretion-phase SN model was performed with the Prometheus-Vertex code as in Ref. [29], using now a $15\,M_\odot$ progenitor [30]. The transport module of the code computes the energy and angle distributions of ν and $\bar\nu$ of all flavors by a tangent-ray discretization of the Boltzmann transport equation [33]. We used 21 nearly geometrically spaced energy bins up to 380 MeV and 672 tangent rays for the discussed model. We do not artificially trigger an explosion because our interest is limited to the accretion phase, but otherwise our model is comparable to Ref. [22]. We use several snapshots and illustrate our findings with one taken at 280 ms post bounce. The flux spectra (Fig. 1) show a ν_e excess from deleptonization and a $\bar\nu_e$ flux almost twice that of ν_x (representing any of $\nu_{\mu,\tau}$ or $\bar\nu_{\mu,\tau}$) and average ν_e, $\bar\nu_e$ and ν_x energies of 15.3, 18.1, and 16.9 MeV.

We study neutrino propagation in the free-streaming limit, so we can describe the angular distribution by the angle ϑ_R relative to the radial direction at a chosen inner-boundary radius R. Actually it is more convenient to use $u = \sin^2\vartheta_R = (1-\cos^2\vartheta_r)\,r^2/R^2$, which is uniformly distributed on $0 \le u \le 1$ if emission is isotropic at a "neutrino sphere" with radius R [21, 28]. We choose $R = 44.7$ km and show the corresponding u distribution in Fig. 1. Isotropic emission from a neutrino sphere is

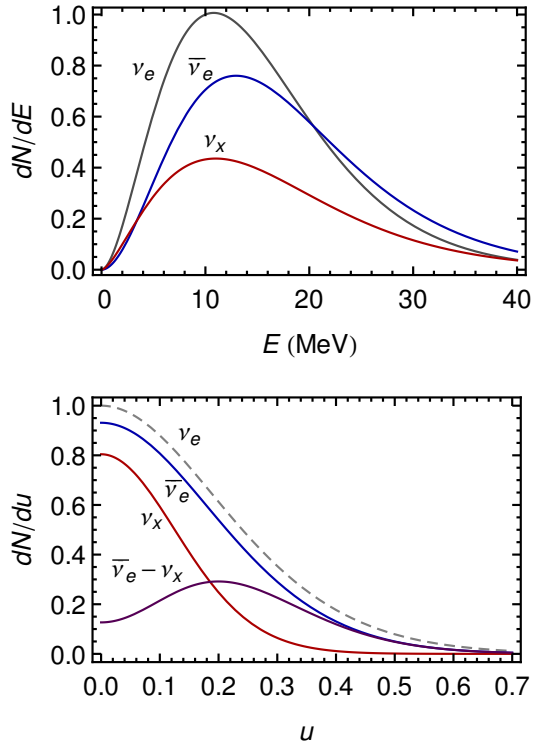

FIG. 1: Flux spectra for our 280 ms SN model. The angle variable $0 \leq u \leq 1$ is based on $R = 44.7$ km.

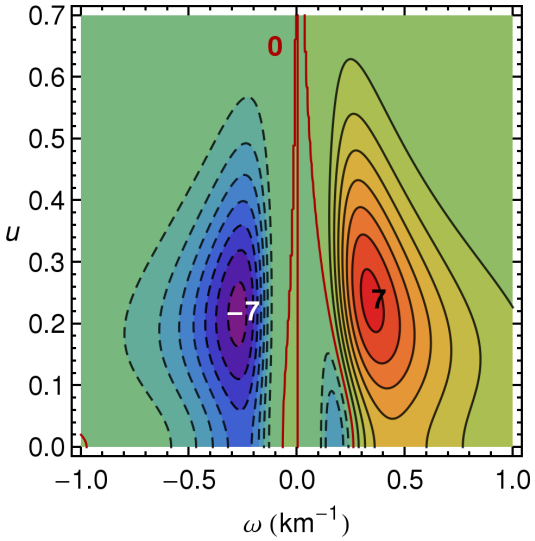

FIG. 2: Distribution $g(\omega, u)$ describing the neutrino fluxes.

not a good description because neutrinos emerge from a thick layer. The $\bar{\nu}_e$ and ν_x intensities are similar in the radial direction: the excess $\bar{\nu}_e$ flux largely arises from its broader angular distribution (larger emission region). Flavor oscillations depend on the difference of the e and x distributions, which is small in the radial direction (Fig. 1). The angular distributions do not cross, although in principle there could have been a forward ν_x excess.

In the context of neutrino oscillations, $\omega = \Delta m^2/2E$ is a preferred energy variable, where $\Delta m^2 = (50\ \text{meV})^2$ is the "atmospheric" neutrino mass-squared difference relevant for 1–3 oscillations studied here. Moreover, treating anti-neutrinos formally as negative-energy neutrinos with negative occupation numbers vastly simplifies the formalism. Flavor oscillations can exchange ν_e with ν_x, leaving the overall neutrino flux unchanged, so only $F_{\nu_e} - F_{\nu_x}$ matters. Our sign convention means that for anti-neutrinos we then use $F_{\bar{\nu}_x} - F_{\bar{\nu}_e}$, corresponding to the flavor isospin convention [14]. The neutrino flux difference distribution $g(\omega, u)$ thus defined is shown in Fig. 2. It is negative for anti-neutrinos ($\omega < 0$) because $F_{\bar{\nu}_e} > F_{\bar{\nu}_x}$. For $\omega \sim 0.2$ km^{-1} there is a spectral crossing as a function of u, i.e. for large E the ν_x flux does exceed the ν_e flux in the forward direction.

Self-induced oscillations exchange the positive and negative parts of $g(\omega, u)$, leaving fixed the overall flavor content $\varepsilon = (F_{\nu_e} - F_{\nu_x})/(F_{\bar{\nu}_e} - F_{\nu_x}) - 1 = \int d\omega\, du\, g(\omega, u)$. Our $g(\omega, u)$ is mostly negative for anti-neutrinos and mostly positive for neutrinos, so collective oscillations largely correspond to pair conversions $\nu_e\bar{\nu}_e \leftrightarrow \nu_x\bar{\nu}_x$. Accretion-phase distributions are "single crossed" in this sense, i.e. $g(\omega, u)$ changes sign essentially only on the line $\omega = 0$, because of the large excess of the ν_e and $\bar{\nu}_e$ fluxes. Significant multiple crossings are typical for the cooling phase [15].

Equations of motion (EoM).—We describe three-flavor neutrino propagation by energy- and angle-dependent 3×3 matrices $\mathsf{\Phi}_{E,u}(r)$. Sans-serif letters denote matrices in flavor space. The diagonal $\mathsf{\Phi}_{E,u}$ elements are the ordinary number fluxes $F^{\alpha}_{E,u}$ (flavor α) integrated over a sphere of radius r. Negative E and negative number fluxes for anti-neutrinos. The off-diagonal elements, which are initially zero, represent phase information caused by flavor oscillations. The flavor evolution is then provided by the "Schrödinger equation" $\mathrm{i}\partial_r \mathsf{\Phi}_{E,u} = [\mathsf{H}_{E,u}, \mathsf{\Phi}_{E,u}]$ with the Hamiltonian [21]

$$\mathsf{H}_{E,u} = \frac{1}{v_u}\left(\frac{\mathsf{M}^2}{2E} + \sqrt{2}\,G_{\rm F}\mathsf{N}_\ell\right) + \frac{\sqrt{2}\,G_{\rm F}}{4\pi r^2}\int_{-\infty}^{+\infty} dE' \int_0^1 du' \frac{1 - v_u v_{u'}}{v_u v_{u'}}\,\mathsf{\Phi}_{E',u'}\,. \tag{1}$$

The matrix M^2 of neutrino mass-squares causes vacuum flavor oscillations and that of net charged lepton densities $\mathsf{N}_\ell = \mathrm{diag}(n_e - n_{\bar{e}}, n_\mu - n_{\bar{\mu}}, n_\tau - n_{\bar{\tau}})$ adds the Wolfenstein matter effect. The third term provides neutrino-neutrino refraction and is analogous to matter except for Pantaleone's off-diagonal elements and except that in the SN context neutrinos are not isotropic. A neutrino radial velocity at radius r is $v_u = (1 - u\,R^2/r^2)^{1/2}$. The factor $1 - v_u v_{u'}$ arises from the current-current nature of the weak interaction and causes multi-angle effects. Moreover, v_u appears in the denominator because we follow the flavor evolution projected on the radial direction,

causing the multi-angle matter effect [21].

Up to the MSW region, the matter effect is so large that $\Phi_{E,u}$ is very nearly diagonal in the weak-interaction basis, the usual approximation made in SN neutrino transport. Neutrinos remain stuck in flavor eigenstates unless the off-diagonal $\Phi_{E,u}$ elements start growing by the self-induced instability. To find the latter we linearize the EoM in the small off-diagonal amplitudes.

Stability condition.—We study the instability driven by the atmospheric Δm^2 and the mixing angle $\Theta_{13} \ll 1$, we work in the two-flavor limit, and switch to the $\omega = \Delta m^2/2E$ variable. We write the flux matrices in the form

$$\Phi_{\omega,u} = \frac{\mathrm{Tr}\,\Phi_{\omega,u}}{2} + \frac{F^e_{\omega,u} - F^x_{\omega,u}}{2} \begin{pmatrix} s_{\omega,u} & S_{\omega,u} \\ S^*_{\omega,u} & -s_{\omega,u} \end{pmatrix}, \quad (2)$$

where $F^{e,x}_{\omega,u}$ are the flavor fluxes at the inner boundary radius R. The flux summed over all flavors, $\mathrm{Tr}\,\Phi_{\omega,u}$, is conserved in our free-streaming limit. The ν_e survival probability is $\frac{1}{2}[1 + s_{\omega,u}(r)]$ in terms of the "swap factor" $-1 \leq s_{\omega,u}(r) \leq 1$. The off-diagonal element $S_{\omega,u}$ is complex and $s^2_{\omega,u} + |S_{\omega,u}|^2 = 1$.

The small-amplitude limit means $|S_{\omega,u}| \ll 1$ and to linear order $s_{\omega,u} = 1$. Assuming in addition a large distance from the source so that $1 - v_r \ll 1$, the evolution equation linearized in $S_{\omega,u}$ and in u is [28]

$$\begin{aligned} \mathrm{i}\partial_r S_{\omega,u} &= [\omega + u(\lambda + \varepsilon\mu)]\, S_{\omega,u} \\ &\quad - \mu \int du'\, d\omega'\, (u + u')\, g_{\omega' u'}\, S_{\omega',u'}\,. \end{aligned} \quad (3)$$

Weak-interaction effects are encoded in the r-dependent parameters with dimension energy

$$\begin{aligned} \lambda &= \sqrt{2}\, G_{\mathrm{F}}\, [n_e(r) - n_{\bar{e}}(r)]\, \frac{R^2}{2r^2}\,, \\ \mu &= \frac{\sqrt{2}\, G_{\mathrm{F}}\, [F_{\bar{\nu}_e}(R) - F_{\bar{\nu}_x}(R)]}{4\pi r^2}\, \frac{R^2}{2r^2}\,. \end{aligned} \quad (4)$$

The factor $R^2/2r^2$ signifies that only the multi-angle impact of both matter and neutrino-neutrino effects enter, and not the electron or neutrino densities themselves. Both λ and μ depend on the chosen R, but also the occupied u range: physical results do not depend on R. We normalize the neutrino-neutrino interaction strength μ to the $\bar{\nu}_e - \bar{\nu}_x$ flux difference at R, i.e. $\int_{-\infty}^{0} d\omega \int_0^1 du\, g_{\omega,u} = -1$, but the only physically relevant quantity is $\mu(r)\, g_{\omega,u}$. Our SN model provides $\mu(R) = 3.45 \times 10^4$ km^{-1} after choosing $R = 44.7$ km. The "asymmetry" is $\varepsilon = \int d\omega\, du\, g_{\omega,u} = 0.35$.

Writing solutions of the linear differential equation, Eq. (3), in the form $S_{\omega,u} = Q_{\omega,u}\, e^{-\mathrm{i}\Omega r}$ with complex frequency $\Omega = \gamma + \mathrm{i}\kappa$ and eigenvector $Q_{\omega,u}$ leads to the eigenvalue equation [28],

$$(\omega + u\bar{\lambda} - \Omega)\, Q_{\omega,u} = \mu \int du'\, d\omega'\, (u + u')\, g_{\omega' u'}\, Q_{\omega',u'}\,, \quad (5)$$

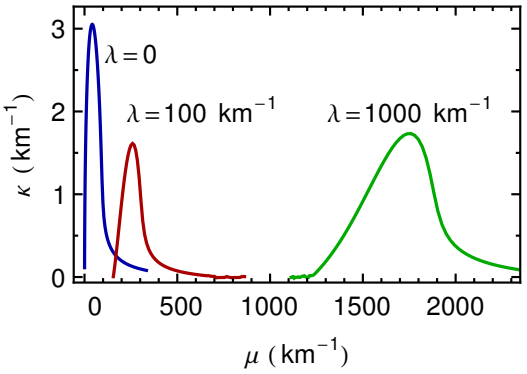

FIG. 3: Growth rate κ for our SN model as a function of μ for various λ values as indicated.

where $\bar{\lambda} \equiv \lambda + \varepsilon\mu$. The solution has to be of the form $Q_{\omega,u} = (A + Bu)/(\omega + u\bar{\lambda} - \Omega)$. Solutions exist if $\mu^{-1} = I_1 \pm \sqrt{I_0 I_2}$, where $I_n = \int d\omega\, du\, g_{\omega,u}\, u^n/(\omega + u\bar{\lambda} - \Omega)$. The system is stable if all Ω are purely real. A possible imaginary part, κ, is the exponential growth rate.

Application to our SN model.—Ignoring the effect of matter ($\lambda = 0$), we show $\kappa(\mu)$ for our 280 ms SN model in Fig. 3. The system is essentially stable above μ of a few 100 km^{-1}. It is noteworthy that κ is of the same order as a typical ω of the $g_{\omega,u}$ distribution, in our case a few km^{-1}. We also show $\kappa(\mu)$ for $\lambda = 10^2$ and 10^3 km^{-1} and observe a shift to larger μ-values [28].

In Fig. 4 we show contours of κ in the (μ, λ) plane. For large μ and λ values, the system is unstable for $\lambda \sim \mu$ [28]. In other words, if the local neutrino number density is much smaller or much larger than the local electron

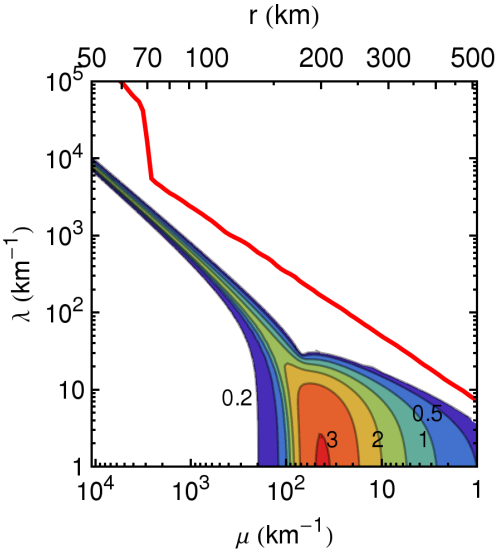

FIG. 4: Contours for the growth rate κ in km^{-1}. Also shown is the profile for our 280 ms SN model. The vertical axis essentially denotes the density, the horizontal axis the radius ($\mu \propto r^{-4}$).

density, the system is stable.

We also show the locus of $[\mu(r), \lambda(r)]$ along the radial direction. Since $\mu(r) \propto r^{-4}$, the red solid line in Fig. 4 is essentially the SN density profile. The step-like feature is the shock wave where the matter density drops by about an order of magnitude. Without matter ($\lambda = 0$), neutrinos would enter the instability strip at $\mu \sim 100$, corresponding to $r \sim 150$ km. We find similar results for other snapshots at times 150 and 400 ms postbounce, i.e., neutrinos do not encounter a self-induced instability.

Comparison with earlier work.—A similar accretion-phase model of the Basel group was used to study flavor stability by numerically solving the EoMs [22]. A mono-energetic neutrino distribution and isotropic emission at a neutrino sphere were assumed. For some snapshots, an instability occurred at a large radius. Applying our method to the same matter profile and schematic neutrino distribution we find perfect agreement with Ref. [22] and even reproduce their onset radius for those cases where partial flavor conversion occurs [31]. It would be interesting to repeat our study with realistic Basel distributions to see if partial flavor conversion is an artifact of their schematic energy and angle distributions.

Conclusions.—We have performed a linearized flavor stability analysis of an accretion-phase SN model and concomitant neutrino fluxes with realistic energy and angle distributions. For the studied models, self-induced flavor conversions do not occur. One should apply this method to a broader class of models to see if our conclusion is generic. It also remains to extend a linearized analysis to cases without cylindrical symmetry of the angular distribution in view of Sawyer's concerns about a significant multi-angle instability [13]. In realistic 3D models, the neutrino distribution is not cylindrically symmetric and even if this were the case, in principle even a small fluctuation could trigger a novel instability if it were to exist.

Recent experimental evidence suggests that the neutrino mixing angle Θ_{13} is not very small [23], a point that should become clear with the ongoing round of reactor and long-baseline experiments. In this case one can distinguish the neutrino mass hierarchy in a high-statistics SN neutrino signal by the presence or absence of Earth matter effects, but only if collective oscillations do not exchange flavors before the MSW region. If the collective flavor swap were fully operational, the mass hierarchy could be distinguished for an extremely small value of Θ_{13} where the MSW conversion is no longer adiabatic [32]. If Θ_{13} is "large" in this sense, the absence of collective flavor oscillations during the SN accretion phase, if generic, is good news.

We thank T. Hahn for helping to implement a numerical library [34]. We acknowledge partial support by DFG Grants No. TR 7, TR 27, EXC 153 and computer time at the HLRS in Stuttgart and NIC in Jülich.

[1] H.-T. Janka, K. Langanke, A. Marek, G. Martínez-Pinedo and B. Müller, Phys. Rept. **442**, 38 (2007).
[2] D. Autiero *et al.*, JCAP **0711**, 011 (2007).
[3] M. Wurm *et al.*, arXiv:1104.5620.
[4] K. Scholberg, J. Phys. Conf. Ser. **203**, 012079 (2010).
[5] A. S. Dighe and A. Y. Smirnov, Phys. Rev. D **62**, 033007 (2000).
[6] L. Wolfenstein, Phys. Rev. D **17**, 2369 (1978).
[7] S. P. Mikheev and A. Yu. Smirnov, Sov. J. Nucl. Phys. **42**, 913 (1985) [Yad. Fiz. **42**, 1441 (1985)]; Sov. Phys. JETP **64**, 4 (1986) [Zh. Eksp. Teor. Fiz. **91**, 7 (1986)].
[8] T. K. Kuo and J. T. Pantaleone, Rev. Mod. Phys. **61**, 937 (1989).
[9] J. Pantaleone, Phys. Lett. B **287**, 128 (1992).
[10] G. Sigl and G. Raffelt, Nucl. Phys. B **406**, 423 (1993).
[11] S. Samuel, Phys. Rev. D **48**, 1462 (1993); Phys. Rev. D **53**, 5382 (1996). V. A. Kostelecký and S. Samuel, Phys. Lett. B **318**, 127 (1993); Phys. Rev. D **52**, 621 (1995).
[12] R. F. Sawyer, Phys. Rev. D **72**, 045003 (2005).
[13] R. F. Sawyer, Phys. Rev. D **79**, 105003 (2009).
[14] H. Duan, G. M. Fuller, J. Carlson and Y.-Z. Qian, Phys. Rev. D **74**, 105014 (2006).
[15] B. Dasgupta, A. Dighe, G. Raffelt and A. Yu. Smirnov, Phys. Rev. Lett. **103**, 051105 (2009).
[16] H. Duan, G. M. Fuller and Y.-Z. Qian, Annu. Rev. Nucl. Part. Sci. **60**, 569 (2010).
[17] B. Dasgupta, E. P. O'Connor and C. D. Ott, arXiv: 1106.1167. Y. Suwa, K. Kotake, T. Takiwaki, M. Liebendörfer and K. Sato, Astrophys. J. **738**, 165 (2011).
[18] H. Duan, G. M. Fuller, J. Carlson and Y.-Z. Qian, Phys. Rev. Lett. **100**, 021101 (2008).
[19] B. Dasgupta, A. Dighe, A. Mirizzi and G. G. Raffelt, Phys. Rev. D **77**, 113007 (2008).
[20] J. F. Cherry, M. R. Wu, J. Carlson, H. Duan, G. M. Fuller and Y.-Z. Qian, arXiv:1108.4064.
[21] A. Esteban-Pretel, A. Mirizzi, S. Pastor, R. Tomàs, G. G. Raffelt, P. D. Serpico and G. Sigl, Phys. Rev. D **78**, 085012 (2008).
[22] S. Chakraborty, T. Fischer, A. Mirizzi, N. Saviano and R. Tomàs, Phys. Rev. D **84**, 025002 (2011).
[23] G. L. Fogli, E. Lisi, A. Marrone, A. Palazzo and A. M. Rotunno, arXiv:1106.6028.
[24] H. Duan, G. M. Fuller and J. Carlson, Comput. Sci. Dis. **1**, 015007 (2008).
[25] S. Hannestad, G. Raffelt, G. Sigl and Y. Y. Y. Wong, Phys. Rev. D **74**, 105010 (2006); Erratum ibid. **76**, 029901 (2007).
[26] H. Duan, G. M. Fuller, J. Carlson and Y. Z. Qian, Phys. Rev. D **75**, 125005 (2007).
[27] G. G. Raffelt, Phys. Rev. D **83**, 105022 (2011).
[28] A. Banerjee, A. Dighe and G. Raffelt, arXiv:1107.2308.
[29] L. Hüdepohl, B. Müller, H.-T. Janka, A. Marek and G. G. Raffelt, Phys. Rev. Lett. **104**, 251101 (2010); Erratum ibid. **105**, 249901 (2010).
[30] S. E. Woosley, T. A. Weaver, Astrophys. J. Suppl. **101**, 181 (1995).
[31] S. Sarikas, Proc. HANSE 2011, in preparation.
[32] B. Dasgupta, A. Dighe and A. Mirizzi, Phys. Rev. Lett. **101**, 171801 (2008).
[33] M. Rampp, H. T. Janka, Astron. Astrophys. **396**, 361 (2002).
[34] T. Hahn, Comput. Phys. Commun. **168**, 78 (2005).